Inorganic Chemistry

Article

pubs.acs.org/IC

Lithium Dihydroborate: First-Principles Structure Prediction of $LiBH_2$

Riccarda Caputo*,† and Adem Tekin‡

†ETH Zürich, Swiss Federal Institute of Technology, Department of Chemistry and Applied Biosciences, Lab Inorganic Chemistry, Wolfgang-Pauli Strasse 10, CH-8093 Zürich, Switzerland

‡Istanbul Technical University, Informatics Institute, 34469 Maslak, Istanbul, Turkey

Supporting Information

ABSTRACT: We report a first-principles structure prediction of the $LiBH_2$, which structures are modeled by using four formula units per unit cell without symmetry restrictions. The computational methodology combines a simulated annealing approach and density functional total energy calculations for crystalline solid structures. The predicted lowest energy structure shows the formation of linear anionic chains, $^1_\infty[BH_2]$, enthalpy of formation at 0 K equal to −90.07 kJ/mol. Ring structures, in particular with butterfly and planar square topologies, are found to be stable but well above the ground state by 20.26 and 12.92 kJ/mol, respectively. All convergent structures fall in the symmetry families monoclinic, tetragonal, and orthorhombic. For the representative structures of each family group, simulated X-ray diffraction patterns and infrared spectra are reported.

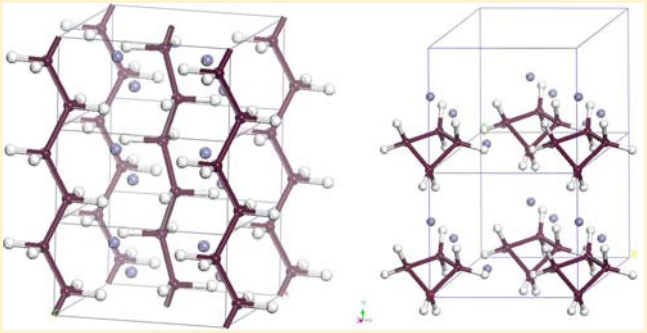

INTRODUCTION

Any potential material used to store hydrogen for onboard applications must be qualified in terms of high density, good reversibility, and fast absorption and desorption of hydrogen kinetics. An attractive class of materials is complex borohydrides especially due to their high volumetric and gravimetric hydrogen density. The lightest complex borohydride is lithium borohydride ($LiBH_4$) with 121 kg H/m^3 and 18.5 wt % H storage capabilities. However, its use is strictly limited by the poor reversibility and requirement for very high decomposition temperatures. According to our best knowledge to date, the decomposition products are not identified quantitatively and qualitatively as already highlighted in ref 1. However, one of the earliest pyrolysis experiment conducted by Schlesinger and Brown[2] indicated that hydrogen evolves in three stages. In the first stage, they examined no volatile material other than hydrogen. Simple stoichiometry consideration for this reaction step reveals that the remaining residue may contain $LiBH_x$ with $x = 2$ or 2.5.

The present work regards the continuation of our theoretical investigation[1] of the possible structures energetically accessible formed by Li, B, and H with atomic ratio 1:1:x, $x \leq 4$. In particular, we considered in the present work the case $x = 2$, with a formula unit $LiBH_2$, which was already discussed elsewhere[1] and suggested therein as a possible candidate structure of the partial decomposition of $LiBH_4$. Whether the thermal decomposition of $LiBH_4$ proceeds via formation of linear chains of lithium hydroborates or via lithium borides with a certain content of hydrogen absorbed in is still a debated question. The possibility to form chains of borohydrides has been already discussed in the past,[3−5] and the remarkable stability of $LiBH_2$ has been studied as single dimer by using ab initio calculations and varying topology via a group theory approach. Recently, interest has been renewed because of widespread research on $LiBH_4$ and its products of partial thermal decomposition.[1,5,6] Urging experimental validation and identification of possible compounds of $LiBH_x$ with $x < 4$ stoichiometry, we report here crystal structure prediction using first-principles methods, following the general methodological approach described elsewhere.[1,7−10]

Because of being formed by charged groups, namely, $Li^{\delta+}$ and $-(BH_2)-^{\delta-}$, after the Coloumb energy, the most long-range contribution to the total energy in $LiBH_2$ is the dispersion term. The weak van der Waals forces play an important role in the stabilization of both ionic and covalent systems. These forces can be included via a nonlocal van der Waals density functional (vdW-DF)[11−13] or the empirical dispersion correction (DFT-D), proposed by Grimme and others.[14,15] The effect of dispersion interaction may also change the relative stability of structures as recently reported for $Mg(BH_4)_2$.[16]

COMPUTATIONAL METHODOLOGY

The general methodological approach completely from first-principles structure modeling and prediction follows the same scheme as already reported.[7−10] The initial model structure was found by analysis of the normal modes of vibration of the orthorhombic structure of $LiBH_4$, as reported.[1] It helped to extract the key information for starting with the subsequent systematic model structure, containing the preferred B−H, B−B, Li−H, and Li−B distances. The bond distances and the

Received: May 29, 2012
Published: August 28, 2012

 © 2012 American Chemical Society dx.doi.org/10.1021/ic301127q | Inorg. Chem. 2012, 51, 9757−9765

Table 1. Symmetry Group (No.), Lattice Parameters (Å), Monoclinic Angle β (deg), Molar Volumes (cm^3/mol), and Enthalpy of Formation (kJ/mol) of the Lowest Energy Structures Belonging to Each Crystal Family Reported in Figure 1[a]

symmetry group (IT)	a	b	c (β)	V_m	$\Delta_f H(0K)$	remarks
			Monoclinic			
$P2_1/c$ (14)	7.267	4.416	8.485 (147.30)	22.148	−52.70	$[BH_2-BH_2]$ fragment
Pm (6)	4.560	3.161	8.949 (85.599)	19.364	−79.72	-(BH_2)- chain (Figure 2) $[B_4H_8]$ butterfly (Figure 5) $[B_4H_8]$ planar square (Figure 6)
$P2/c$ (13)	13.907	10.057	9.465 (11.195)	19.345	−66.92	
Cc (9)	7.002	6.812	5.706 (113.822)	18.745	−90.07	
Cm (8)	8.489	7.075	5.695 (101.013)	25.272	−69.81	
$C2/m$ (12)	8.295	5.379	6.049 (117.531)	18.014	−77.15	
			Orthorhombic			
$Cmcm$ (63)	3.907	8.692	3.188	16.299	−75.67	BH_2- chain (Supplementary Figure 4, Supporting Information) BH_2- chain (Figure 4) BH_2- chain
$Pnma$ (62)	5.946	3.124	6.298	17.614	−88.07	
$P222_1$ (17)	4.842	4.883	5.320	18.937	−86.24	
			Tetragonal			
$P4_2/mnm$ (136)	6.244	6.244	3.874	22.738	−65.25	2*$[BH_2-BH_2]$ fragment
$P4/mbm$ (127)	6.052	6.052	6.065	33.445	−54.09	
$P4_322$ (95)	5.236	5.236	4.767	19.677	−85.77	-(BH_2)- chain (Figure 3)

[a]The lattice parameters of the orthorhombic structure, *Pnma*, are comparable to those reported by Kolmogorov et al.[5]

coordinations of Li atoms represent the piece of information to perform simulated annealing (SA) calculations and consequently to scan the phase space of possible molecular arrangements, with Li/B/H atomic ratio 1:1:2. Global optimizations are performed by maximizing the number of Li−H bonds within a (2 × 2 × 2) cut-through lattice using only bond length constraints and four formula units (f.u.) of $LiBH_2$. One of the lithium atoms is set at the origin; the other ones, as well as BH_2 groups, are located using spherical coordinates. More details about the parametrization of the model can be found elsewhere.[8] Inclusion of bond length constraints into the model serves to mimic the repulsive interactions between atom pairs. Based on this scheme, a crystal structure is accepted if the following distance criteria are fulfilled: the distances between Li−Li, B−B, Li−B, and H−H in the (2 × 2 × 2) cut-through lattice must be longer than 3.22, 1.8, 2.16, and 2.33 Å, respectively. In addition to this set, the following alternatives are also used to obtain a refined selection of the possible structures on the potential energy surface (PES): (2.85, 1.63, 2.12, 2.33 Å) and (3.22, 1.7, 2.16, 2.33 Å). The total number of Li−H bonds in the cut-through lattice, which is the objective function in the SA optimizations, are determined by counting the bonds satisfying the following ranges: 2.4−1.8 Å for the first and the last distance sets and 1.8−1.9 Å for the second set. All these threshold sets were obtained with the help of the structure reported in ref 1. Employing these threshold sets, the SA algorithm has been started 500 times for each different type of unit cell. For the periodic lattice optimization, we employed density functional theory (DFT) calculations, in particular CASTEP,[17] implemented in Materials Studio 5.5. We use norm-conserving pseudopotentials for all atoms and a fine mesh of k points, commensurate to the specific lattice dimensions, but with the actual spacing below 0.03 $Å^{-1}$. The energy threshold is set to 0.01 meV/atom, the maximum atomic displacement to 0.001 Å, and the maximum atomic force threshold at 0.001 eV/ Å. We use the Perdew−Burke−Ernzerhof96 and the generalized gradient form (GGA-PBE) of the exchange−correlation functional. Noncovalent forces and in particular van der Waals interactions are introduced by using damped atom-pairwise dispersion corrections of the form C_6R^{-6}, proposed by Grimme,[14] as implemented in CASTEP. Density functional perturbation theory (DFPT) by using CASTEP[17] is employed for phonon calculations. The simulated infrared (IR) spectra are calculated by using the property analysis implemented in Materials Studio5.5. Furthermore, the Reflex powder diffraction module, in Materials Studio5.5, is used to simulate the XRD patterns of the optimized structures. In the simulations, we use the X-ray radiation for a Cu source with λ_1 = 1.5405 Å.

RESULTS AND DISCUSSION

In a previous work,[1] we reported model structures of the partial thermal decomposition of $LiBH_4$, focusing on those that might be formed via desorption of adjacent hydrogen atoms, forming molecular hydrogen. Therein the two model structures proposed, namely, $LiBH_2$ and $LiBH_{2.5}$, were generated by considering the vibrational spectra of several $LiBH_4$ structures.[8] In the present study, we systematically investigated the stability of structures allowing for a formula unit of $LiBH_2$ by using the computational approach that was already successfully applied for investigating stable structures of metal borohydrides and ammines.[7−10,18] The employed ab initio crystal structure methodology validates the chain structure formation previously suggested,[1] but it allowed us to broaden and explore in more detail the phase space and to identify other possible stable structures with the same atomic ratio.

SA Models. The SA calculations reveal the recurrent topologies adopted by the system of Li, B, and H with the atomic ratios 1:1:2 under the computational settings described before. In fact, in addition to arrangements with a maximum number of Li−H bonds and chains of -(BH_2)- units, we find a ring geometry of boron atoms with triangular and quadrangular arrangements and fragments containing two and four boron atoms. An ensemble of 40 representative structures out of the SA models were selected for the subsequent periodic structure calculations.

Periodic Structures. In principle, given n atoms of boron and 2n atoms of hydrogen in $Li_nB_nH_{2n}$, we can ask how many nonequivalent configurations are geometrically possible. For the sake of simplicity, taking four formula units per unit cell (n = 4), the boron skeleton with four boron atoms can be arranged in different ways: chain, quadrangle, triangle plus one BH_3 group, and fragments containing two or four boron atoms. The chain, formed by a -(BH_2)- repetition, resembles the alkane chain, with the main difference that it has to carry a net negative charge. The triangular configuration with one boron atom bound on one vertex, $B_3H_5(BH_3)$, recalls the recurring three-boron-atom frame of boron-based compounds. The quadrangular structure, B_4H_8, can adopt either a planar square skeleton of boron atoms, each binding two hydrogen atoms, or an out-of-plane, a butterfly geometry. The chain structure,

dx.doi.org/10.1021/ic301127q | Inorg. Chem. 2012, 51, 9757−9765

$^1_\infty[BH_2]$, binding two hydrogen atoms to each boron atom, -($BH_2BH_2BH_2BH_2$)-, can be cut into fragments containing four or two boron atoms by allowing two hydrogen atoms to move on adjacent -(BH_2)- groups and thus leaving the previously bound boron atom with one hydrogen ligand. Accordingly, the hydrogen atoms can be distributed in three different ways on the fragments: $BH_3BHBHBH_3$ or $BH_3BH_2BHBH_2$ on the four-boron atom skeleton, all of which are clearly anionic fragments, and a branched boron skeleton, which, limited to our minimal number of formula units, can be modeled as $BH_3B(BH_2)BH_3$, in which one BH_2 group binds to the central boron atom of a three boron fragment. The triangle skeleton can allocate (2,2,1) hydrogen atoms on the triangle and three on the bound boron atom, resulting in the sequence $BH_2BH_2BH{-}BH_3$. In total, and limited to the minimal four formula units as basis for structure modeling, there are seven nonequivalent topological configurations available to the boron−hydrogen moiety. The number of different periodic structures starting with those configurations is then ruled by the coordination of lithium atoms, which constitute the cations. Generally, as we already highlighted in the study of $LiBH_4$,[8] lithium atoms coordinate in a bidentate way to the hydrogen atoms of a (BH_4) group, even if the tridentate configuration represents the lowest energy state in an isolated Li−BH_4 unit, as also found in $NaBH_4$[9] and the monodentate configuration always leaves the structure at higher energy. Therefore, no monodentate configuration is expected to lead to a stable structure. In fact, none of the 40 optimized structures out of the SA model structures show a monodenate coordination of lithium atoms to hydrogen atoms. All convergent structures optimize into three symmetry group families: monoclinic, tetragonal, and orthorhombic. None of the optimized structures, reported in Table 1, exhibit hexagonal and cubic symmetry. In Figure 1, all structures considered in this study are reported, including those with triclinic symmetry, for which total energies converge in our DFT approach and the corresponding geometries optimize within 0.001 Å tolerance for the atomic positions. The calculated enthalpies of formation

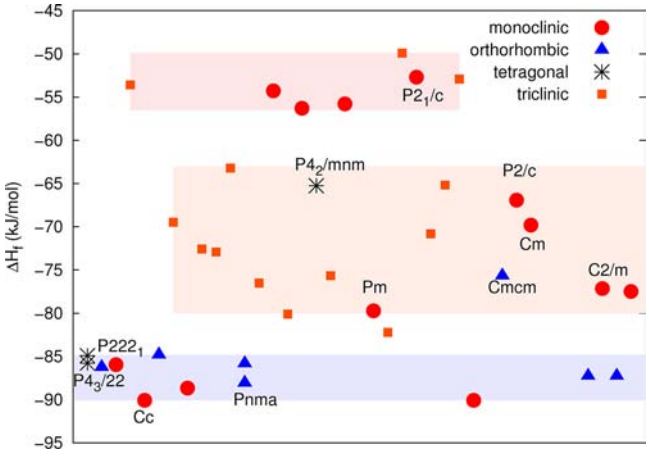

Figure 1. Enthalpies of formation in kJ/mol of the optimized structures. Three general ranges of enthalpy of formation are highlighted. The highest energy structures are all monoclinic and contain $BH_2{-}BH_2$ fragments. The lowest energy structures contain the -(BH_2)- chains. In between, there are those structures showing stressed chains, for example, the chain structure with symmetry $P2/c$ (N0 13) and $\Delta_f H$ = 66.918 kJ/mol and the quadrangular structures, butterfly and planar square configurations, with −69.809 kJ/mol and −77.146 kJ/mol enthalpy of formation, respectively.

without accounting for the zero point energy and the dispersion contributions, and referred to Li(s), body centered cubic structure, α-B(s), and H_2(g), fall in the range (−90.07, −49.91) kJ/mol. Of the structures with broken chains, the $BH_3BHBHBH_3$ configuration has the lowest enthalpy of formation of −82.21 kJ/mol. The short bond length between B_2 and B_3, namely, the boron atoms binding to one hydrogen atom each, is a double bond, as supported by the electron density surface in Supplementary Figure 1, Supporting Information. The structure with $BH_3BH_2BHBH_2$ configuration has a short bond length between the boron atoms of $BH_2{-}BH$. Consequently, they share more electron density, as displayed in Supplementary Figure 2, Supporting Information. The corresponding enthalpy of formation is −75.67 kJ/mol. A slightly more negative enthalpy of formation of −76.51 kJ/mol is found for the structure with the branched boron−hydrogen arrangement, denoted as $BH_3B(BH_2)BH_3$. The optimized boron−boron bond lengths in $BH_3{-}B{-}BH_2BH_3$ are 1.78 Å (BH_3−B), 1.62 Å (BH_2−B), and 1.79 Å (BH_3−B) as displayed in Supplementary Figure 3, Supporting Information. The lowest energy structure, its 3D-view, and the total electron density map are shown in Figure 2; it is monoclinic with symmetry group *Cc* (No 9). It adopts a chain conformation of the -(BH_2)- moieties. The highest energy structure is also monoclinic, but the -(BH_2)- units form a double $[BH_2{-}BH_2]^{-\delta}$ anion per unit cell. Close in energy to the ground-state structure and differing from it by only 1.41 kJ/mol, there is another monoclinic structure with chain configuration, but with *C*2/*c* (No 15) symmetry group. The chain formation, in fact, makes possible the rotation along the B−B bonds, with a consequent change of the symmetry group of the lattice. The B−B−B angle of the boron skeleton is slightly large, 121.3° compared with 117.2° and 120.1° in the lowest energy structure. Consequently, the B−B bond lengths are slightly different, being all equal to 1.809 Å in the higher energy structures and 1.816 and 1.810 Å in the lower energy one. This apparently counterintuitive configuration of the chain finds its justification in the Li−H distances, which are shorter in the lowest energy structure, 1.90, 1.95, 2.02, and 2.99 Å, and 2.00 (x4) or 2.23 Å (x2) in the highest energy structure. Clearly, the lithium coordination to hydrogen atoms, and hence polarization and Coulomb contributions, determine the conformation of the chain. The chain conformation is also present in the tetragonal structures with symmetry group $P4_3$ (No 78) and $P4_322$ (No 95) and in the orthorhombic structures with symmetries $P222_1$ (No 17) and $P2_12_12_1$ (No 19). However, the tetragonal modifications contain helical chiral chains and thus constitute enantiomeric pairs of modifications. In Figure 3, a 3D view of the tetragonal structure, $P4_322$ (No 95), is displayed. The latter structure can change into the orthorhombic *Pnma* (No 62) modification, keeping the chain conformation, without any notable changes of bond lengths and lattice parameters, but with a gain of the total energy of 2.25 kJ/mol. The corresponding enthalpies of formation of those low-energy chain structures, with energies of 2.81 and 5.16 kJ/mol above the ground state, respectively, are displayed in Figure 1. The low-energy orthorhombic structure can be considered to be that with symmetry group *Pnma*. A 3D-view and the total electron density are shown in Figure 4. At 10.36 and 14.40 kJ/mol above the ground state, we found two chain structures with monoclinic *Pm* (No 6) and orthorhombic *Cmcm* (No 63) symmetry groups. A 3D-view and the Li-coordination of the orthorhombic structure are shown in Supplementary Figure 4,

dx.doi.org/10.1021/ic301127q | *Inorg. Chem.* 2012, 51, 9757−9765

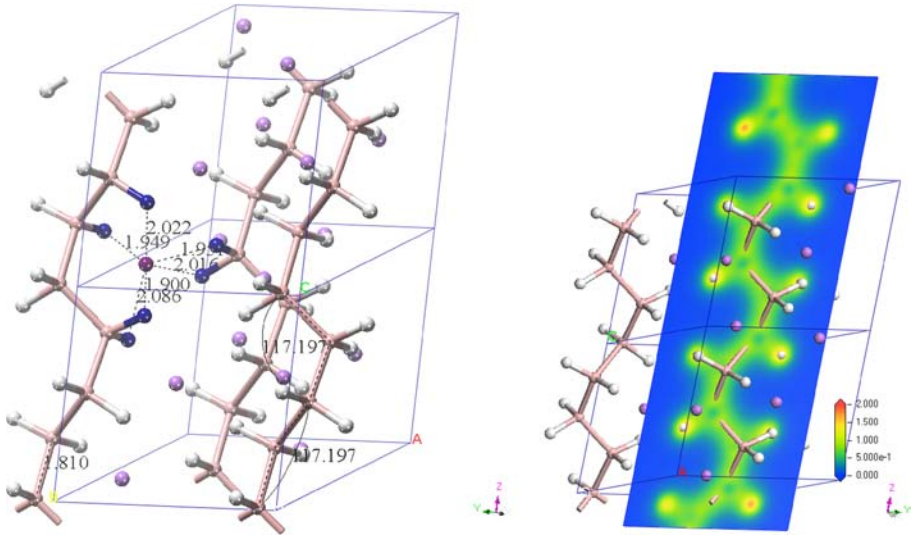

Figure 2. A 3D view of the lowest energy structure with monoclinic *Cc* (No 9) symmetry group. The boron−boron bond lengths are 1.82 and 1.81 Å. The angles in the chain, namely, the angles of the boron−boron skeleton, are 117.97° and 120.09°. The lithium atoms are coordinated to six nearest hydrogen atoms (colored in blue) in the range 1.90−2.09 Å. (right panel) The map of the total electron density projected on a plane passing through the chain. Color scheme: Li, violet; B, pink; H, light gray.

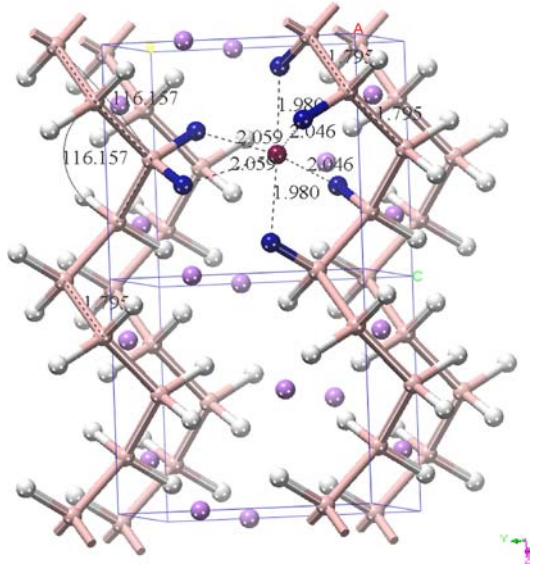

Figure 3. A 3D view of the tetragonal structure with symmetry group $P4_322$ (No 95). All boron−boron bond lengths are equal to 1.79 Å, and the angles in the boron chain are all equal to 116.16°. The lithium atoms are coordinated to six hydrogen atoms (colored in blue) in the distance range 1.98−2.06 Å. Color scheme: Li, violet; B, pink; H, light gray.

Supporting Information. Different from chain structures, we found a ring-(B_4H_8) configuration, which can adopt planar square and butterfly geometries. Their corresponding enthalpies of formation are 12.93 and 20.26 kJ/mol above the ground state, respectively. The corresponding 3D-views are reported in Figures 5 and 6. Structures with higher enthalpy of formation may have, in addition to the chain arrangement of boron−boron bonds, either the formation of anionic fragments with (BH_3) terminal groups or BH_2−BH_2 groups. Interesting is the structure at 23.15 kJ/mol above the ground state, in which the -(BH_2)- chain adopts a pseudo-cis configuration, with a B−B−B angle of 119.4°, Li being coordinated to five hydrogen atoms, one of which is 1.91 Å apart. The energy difference between that structure and the tetragonal $P4_322$ (No 95) structure of 18.85 kJ/mol is probably the reason for the chain stress and the lower coordination of lithium atoms. Furthermore, closing the chain in the butterfly configuration makes the high-energy structure more stable by 2.89 kJ/mol, because the stress in the cis structure is counterbalanced by the formation of an additional B−B bond. The initial model of the high-energy structure with cis configuration was obtained by considering the real normal modes of vibration of the hexagonal $LiBH_4$ structure, following the approach already reported.[1] For higher energy structures, the chain fragmentation and consequently the formation of [BH_2−BH_2] anions prevails on the chain conformation. In fact, close to the highest energy structure, the monoclinic structures, still with symmetry group $P2_1/c$ (No 14) and containing [BH_2−BH_2] groups, differ in energy by 1.58 and 3.59 kJ/mol, due to a different relative alignment of the [BH_2−BH_2]. One of the convergent structures, worthy of being considered in more detail, has orthorhombic symmetry *Pnma* (No 62). That symmetry of $LiBH_2$ was proposed[6] as one of the possible products of the partial decomposition of $LiBH_4$ and a couple of years later studied computationally.[5] Actually, one of the first theoretical studies, to the best of our knowledge, based on cluster models,[4] already reported the exceptional stability of $LiBH_2$. In addition, in our previous work, we mentioned[1] that the interest in $LiBH_2$, or in general $LiBH_x$ with $x \leq 4$, can be motivated by seeking either products or intermediates of the partial decomposition of $LiBH_4$ by the possibility to absorb hydrogen into LiB. Clearly, without entering into the experimental difficulties that might prevent or hinder the formation of a pure crystal phase at different x values, the question that might be addressed from the computational point of view is whether thermodynamically stable modifications of $LiBH_x$ with different x may exist. Our orthorhombic structure of *Pnma* symmetry converges to lattice parameters very similar to those reported in literature.[5] Our first model structure[1] was obtained independently from the literature data, by considering the normal modes of adjacent hydrogen atoms in $LiBH_4$ and the quantitative chemical analysis reported in the pioneering experimental work by

dx.doi.org/10.1021/ic301127q | *Inorg. Chem.* 2012, 51, 9757−9765

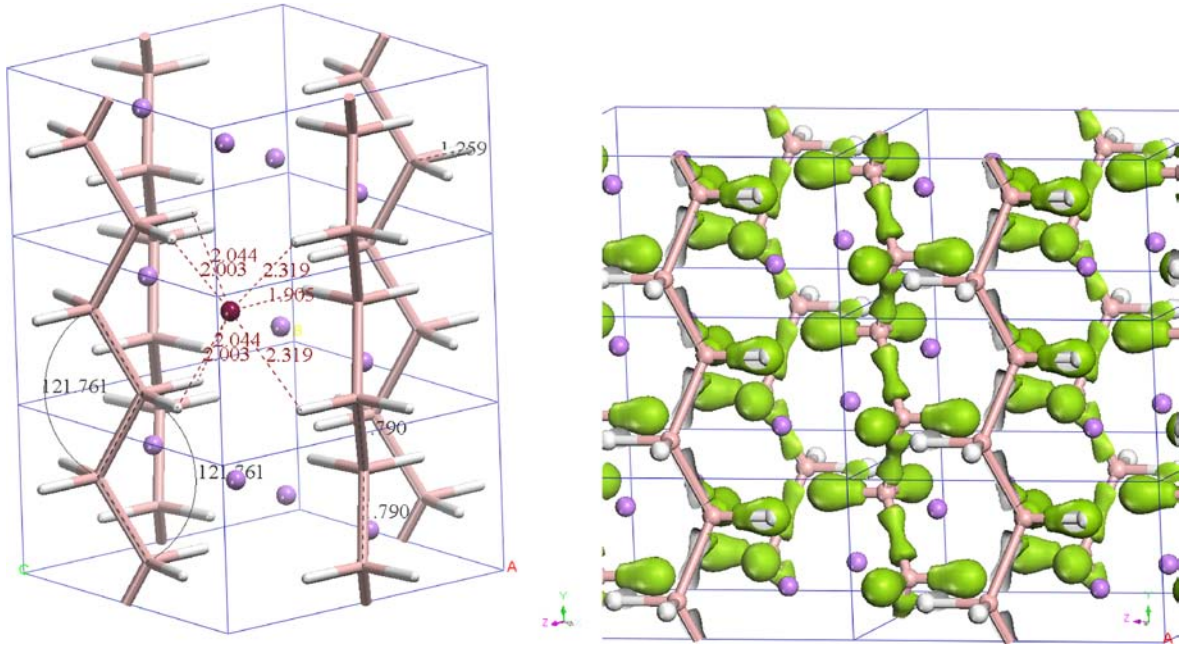

Figure 4. (left panel) A 3D view of the orthorhombic structure, symmetry group *Pnma* (No 62). All boron−boron bond lengths are equal to 1.79 Å. The angles of the boron chain are all equal to 121.76 Å. The lithium atoms are coordinated to five nearest hydrogen atoms at distances in the range 1.91−2.04 Å and two hydrogen atoms belonging to the adjacent chain at 2.32 Å. (right panel) The isodensity surface of the total electron density at 0.80 electrons/Å^3 shows that all B−B bonds are equivalent. Color scheme: Li, violet; B, pink; H, light gray.

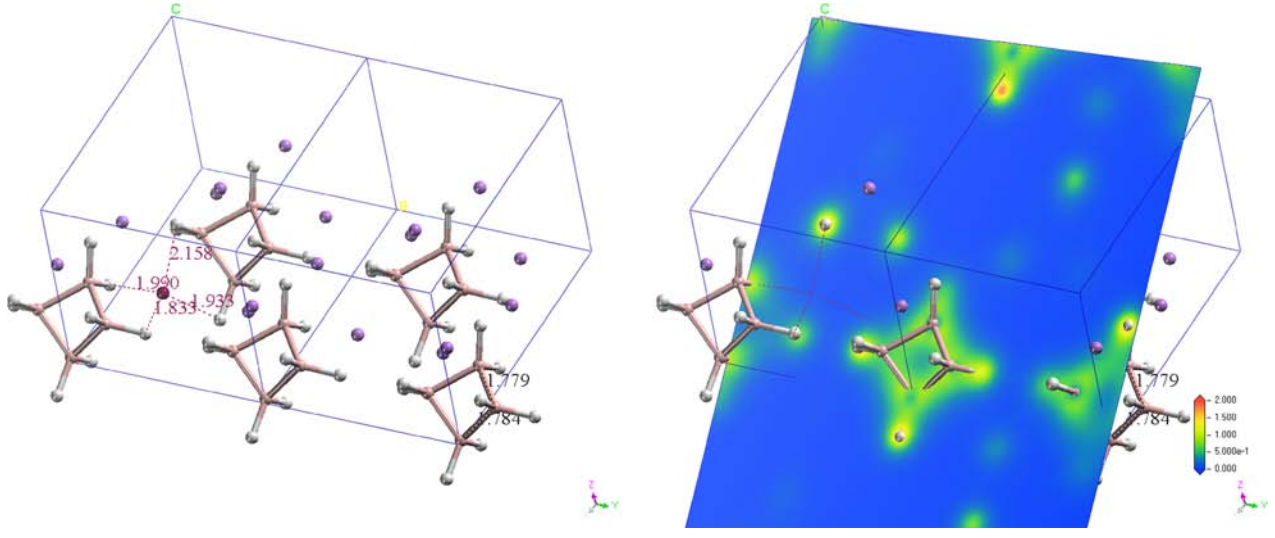

Figure 5. A 3D view of the monoclinic structure, symmetry group *Cm* (No 8) with the ring geometry of the B_4H_8 anions. The boron−boron bond lengths are 1.78 Å. The lithium atoms are coordinated to the nearest hydrogen atoms in the range 1.83−2.16 Å. (right panel) A projection of the total electron density on the plane passing through the ring is shown. Color scheme: Li, violet; B, pink; H, light gray.

Schlesinger.[2] On the other side, in the present work, we checked whether the reported orthorhombic structure[6] converged to one of our model structures. We find that the corresponding enthalpy of formation is positive, clearly suggesting that it cannot represent a stable structure in the theoretical framework, even if the optimized geometry shows the same symmetry group as reported in the reference. By comparison with our model structures of orthorhombic symmetry *Pnma* (No 62), the optimized structure starting with the geometry suggested in literature[6] exhibits a more stressed -(BH_2)- chain with a larger B−B bond length, 1.89 Å compared with 1.79 Å, and smaller B−B−B angle, 106.5°, instead of 121.8°. In addition, the main structural difference between them is the relative orientation of the hydrogen atoms and the sites occupied by lithium atoms. Consequently, it leads us to think that the unstable structure might represent a very high energy state of the lowest one dynamically achievable by torsion along the B−B axes, but it would be highly unlikely because it will require an increase of 12.3% of the lattice volume at the expense of 176.14 kJ/mol. Considering that the required energy would be high and other intermediate stable structures would exhibit a torsion along the B−B bond, we can safely exclude that it might be a possible structure along a minimum energy path of the configurational space. In fact, even including the zero-point energy contribution, none of the stable structures we found would have a positive enthalpy of

dx.doi.org/10.1021/ic301127q | *Inorg. Chem.* 2012, 51, 9757−9765

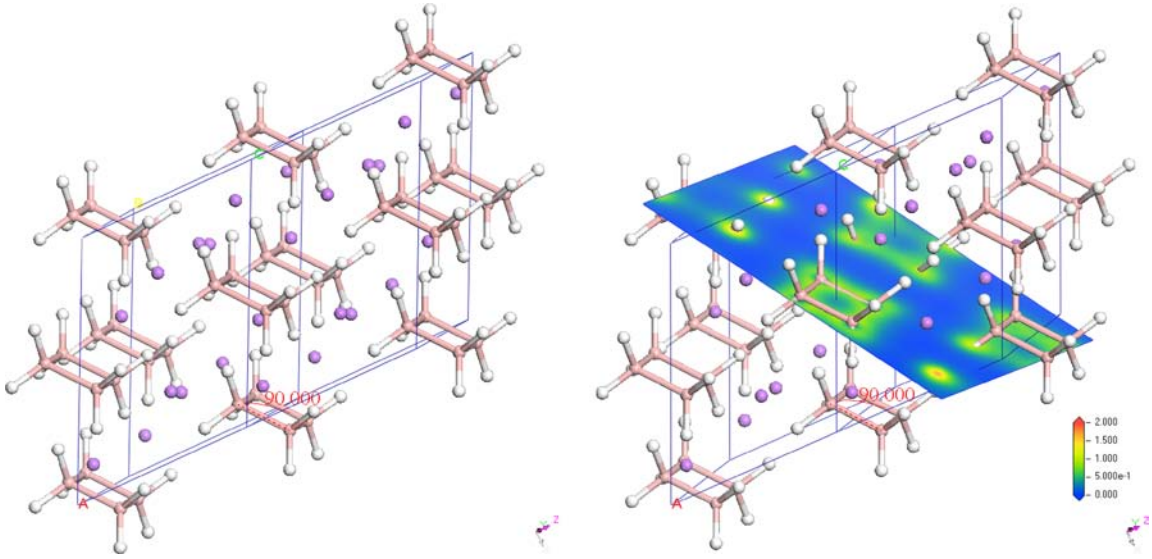

Figure 6. A 3D view of the monoclinic structure, symmetry group $C2/m$ (No 12), with the planar square arrangement of the B_4H_8 anions. The boron−boron bond lengths are all equal to 1.80 Å. The angle of the boron skeleton is 90°, and the angle H−B−H is 103.56°. (right panel) A projection of the total electron density on the plane passing through the ring is shown. The lithium atoms are coordinated to six nearest hydrogen atoms at distances in the range 1.96−2.08 Å. Color scheme: Li, violet; B, pink; H, light gray.

formation. The maximum range of variability with which the zero-point energy contributes is 1.32 kJ/mol, which is the zero-point energy difference of the tetragonal symmetry group No 95 and the square planar structures. The dependence of the enthalpy of formation on the molar volume of selected structures reported in Table 1 and Supplementary Figure 5, Supporting Information, shows that the lowest energy structures with the minimum molar volume have a chain configuration -(BH_2)-, for which the relative orientation of the hydrogen atoms and the exact positions of lithium atoms determine the symmetry group of the structure. Structures with increased molar volume have BH_2−BH_2 fragments and accordingly no more B−B chains are possible. That consistently brings the system to higher energy because two B−B bonds are lost. A regain in energy, 17.11 kJ/mol, is achieved when ring-(B_4H_8) formation is achieved, but with an increased molar volume, 14.11% compared with the highest energy monoclinic structure. For the whole ensemble of selected model structures obtained via SA calculations, we included the dispersion contributions, by using the Grimme scheme implemented in CASTEP. Averaging the total energies of chain structures, by using plain DFT calculations, the mean enthalpy of formation is −86.37 ± 2.76 kJ/mol (standard deviation), the minimum energy structure being that with monoclinic symmetry, *Cc*. Interestingly, by adding the dispersion contribution in the geometry optimizations, we obtain the lowest energy structure for that with orthorhombic symmetry *Pnma* group. Accordingly, the difference $\langle E_{DFT-D}\rangle - \langle E_{DFT}\rangle$, between the mean values of the total energies of chain structures with and without the dispersion contribution, is −90.67 ± 6.44 kJ/mol, which is the difference of the corresponding standard deviations, $\delta(\sigma_{DFT-D} - \sigma_{DFT})$. By accounting for the dispersion term, the DFT-D calculations preferentially lower the total energy of the orthorhombic structure, *Pnma*, overestimating the H−H interaction in the chains and between the adjacent chains. In fact, the two chain structures, monoclinic *Cc*, and orthorhombic *Pnma*, differ by −2.00 kJ/mol using DFT calculations, the monoclinic being lower, but including the dispersion contribution, the orthorhombic is lower than the monoclinic by 15.71 kJ/mol. That difference becomes 18.50 kJ/mol when the corresponding zero-point energy contributions are accounted. Clearly, a complete evaluation of the long-range interaction energy contribution to the total energies, and hence the exact identification of the ground state symmetry group, requires a detailed comparison of the existing semiempirical dispersion−correction schemes and the high-level quantum chemical wave functions methods. Only the DFT-D Grimme scheme is neither sufficient nor conclusive. Therefore, we limit the discussion in the present work to DFT results. Nevertheless, both DFT and DFT-D calculations point out the possibility of chain formation.

Simulated XRD Patterns. It is highly desirable to have experimental data of possible structures of $LiBH_2$, but to our best knowledge, this is not yet reported in literature. Therefore, we think that the simulated XRD patterns of the optimized structures might serve as a guide for the interpretation of the experimental patterns eventually obtained either from the products of partial desorption of H_2 from $LiBH_4$ or from the partial hydrogenation of LiB. In Figure 7, we report the simulated XRD patterns of one of the representative structures for each symmetry family, namely, monoclinic, orthorhombic, and tetragonal. They differ by 6.10 kJ/mol, and all have the chain -(BH_2)-. In Figure 8, the XRD patterns of the planar square and butterfly structures are reported. The geometries of selected chain and ring structures are reported in Tables 2 and 3, respectively.

Phonon Calculations. The structure stabilities are checked by performing the phonon calculations. In particular, we considered the structures with chain, -(BH_2)-, and ring configurations. Independently of the symmetry, either tetragonal or orthorhombic, the structures with chains exhibit all real modes of vibration. Similarly, the ring structures, either butterfly or planar square geometry, exhibit real modes of vibrations. Three characteristic regions are present in all chain and ring structures. The frequencies at low wave numbers describe the cooperative motions of lithium atom and the

dx.doi.org/10.1021/ic301127q | *Inorg. Chem.* 2012, 51, 9757−9765

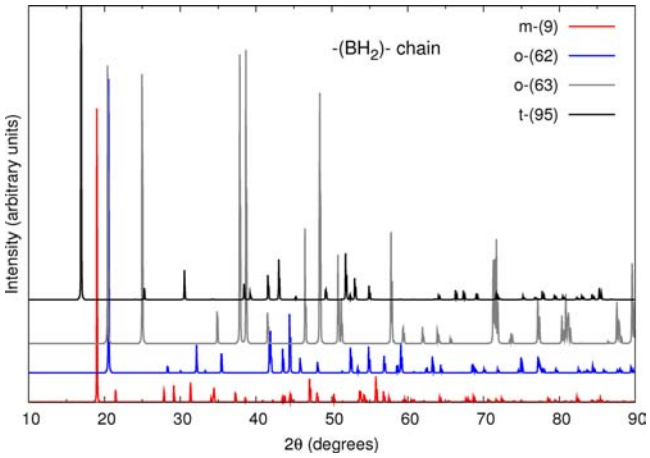

Figure 7. A selection of the simulated XRD patterns of optimized structures with chain formation. The symmetry groups are monoclinic (m), orthorhombic (o), and tetragonal (t).

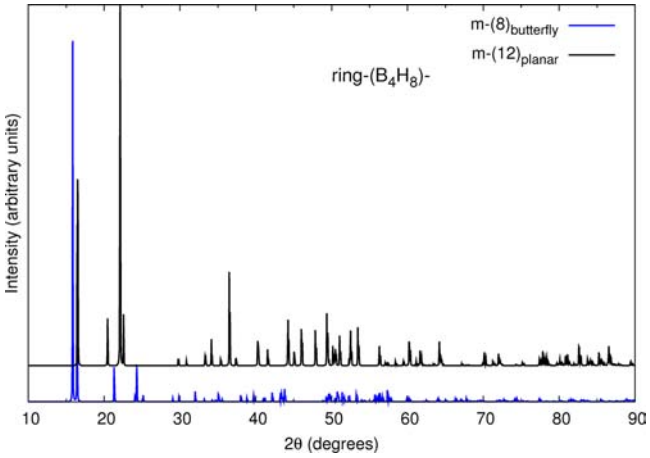

Figure 8. A selection of the simulated XRD patterns of the optimized structures with ring geometry of boron atoms.

nearest neighbor hydrogen atoms. The vibrations in the range 1000−1500 cm^{-1} are the bending motions of B−H bonds. The high wavenumber modes, in the range 2000−2500 cm^{-1}, describe the stretching modes of B−H bonds. Comparing the vibrations of two orthorhombic structure with symmetries $P2_12_12_1$ (No 19) and $P222_1$ (No 17), the increasing symmetry of the structure becomes, of course, visible in the IR spectra, but the two structure can be considered isoenergetic, differing by only 0.42 kJ/mol. The comparison of the two ring structures shows the absence of the stretching mode at 1817.77 cm^{-1} for the planar geometry, which is due to an intense stretching mode of one B−H bond. A bending mode at 1281.74 cm^{-1} of the butterfly configuration is present at 1240.86 cm^{-1} in the planar square. In Figure 9, we report the calculated IR spectra of the structures with chain and the ring configurations of the B_nH_{2n} groups. The results of phonon calculations are used to compute the heat capacity (C_v) as a function of temperature, by numerical integration of the phonon density of states as reported.[19] The integral $\int_{T_1}^{T_2} C_v\, dT$, from lim T_1 = 0 to T_2 = 298.15 K is the thermal contribution to the enthalpy. For the chain structures with orthorhombic symmetry, namely, the ones with symmetry groups Nos. 17, 19, 62, and 63, the thermal contribution is 6.78, 6.06, 7.01, and 6.34 kJ/mol respectively. The corresponding value for the tetragonal structure, symmetry group No 95, is found in the same range to be 6.36 kJ/mol. The thermal contribution of the lowest energy structure *Cc* is 6.17 kJ/mol. Interestingly, the ring structures have a very similar thermal contribution: 6.00 kJ/mol in the square planar configuration and 6.63 kJ/mol in the butterfly configuration. The bending mode of the ring is at 443.89 and 477.99 cm^{-1} in the square planar and butterfly configurations, respectively. The small energy difference between them and the normal modes of vibration of the ring suggest that the two configurations are dynamically connected by overcoming a small energy barrier, which is 7.34 kJ/mol at DFT level.

Table 2. Wyckoff Positions of the Optimized Chain and Ring Structures[a]

atom	*x*	*y*	*z*	site
Monoclinic *Cc* (No 9) -(BH_2)- Chain				
Li	0.2211	0.3357	0.4671	4a
Li	0.2717	0.1702	0.0318	4a
B	0	0.4121	0	4a
B	0.0971	0.5964	0.2505	4a
H	0.0228	0.2485	0.1137	4a
H	0.3031	0.0766	0.3946	4a
H	0.2920	0.5807	0.3449	4a
H	0.5745	0.2660	0.1573	4a
Orthorhombic *Cmcm* (No 63) -(BH_2)- Chain				
Li	0	0.3628	1/4	8g
B	0	0.0505	1/4	4c
H	0.2386	0.1464	1/4	8g
Orthorhombic *Pnma* (No 62) -(BH_2)- Chain				
Li	0.2238	1/4	0.7131	4c
B	0.0542	1/4	0.0468	4c
H	0.0547	1/4	0.2467	4c
H	0.2647	1/4	0.0141	4c
Orthorhombic $P222_1$ (No 17) -(BH_2)- Chain				
Li	0	0.6940	1/4	2c
Li	1/2	0.1633	1/4	2d
B	0	0.1733	1/4	2c
B	0.1832	0	0	2a
H	0.6509	0.1724	0.5904	4e
H	0.1633	0.3371	0.3587	4e
Monoclinic *C*2/*m* (No 12) [B_4H_8] Planar Square				
Li	0.3737	0	0.0914	4i
Li	0.2350	0	0.5450	4i
B	0.0936	0.1678	0.1547	8j
H	0.0623	0.2590	0.3226	8j
H	0.2386	0.2709	0.1890	8j
Monoclinic *Cm* (No 8) [B_4H_8] Butterfly				
Li	0	0.2800	0.0006	4b
Li	0.8525	0	0.2294	2a
Li	0.2967	0	0.4764	2a
B	0.2579	0.1794	0.1036	4b
B	0.1182	0	0.1632	2a
B	0.3029	0	0.8958	2a
H	0.3661	0.2086	0.2802	4b
H	0.2151	0.3453	0.0267	4b
H	0.0661	0	0.3618	2a
H	0	0	0	2a
H	0.4319	0	0.7943	2a
H	0.1905	0	0.7300	2a

[a]The geometry optimizations are obtained using DFT.

dx.doi.org/10.1021/ic301127q | *Inorg. Chem.* 2012, 51, 9757−9765

Table 3. The Tetragonal Structure with Chain Conformation[a]

atom	*x*	*y*	z	site
	Tetragonal $P4_322$ (No 95) or $P4_122$ (No 91)			
Li	0	0.6766	0	4a
B	0	0.1813	0	4a
H	0.1524	0.3309	0.1201	8d
	Tetragonal $P4_3$ (No 78) or P_41 (No 76)			
Li	0.0010	0.3229	0.4998	4a
B	0.0004	0.1811	0	4a
H	0.1538	0.3302	0.1194	4a
H	0.3309	0.1522	0.6305	4a

[a]Wyckoff positions of the standard representation of the two chiral tetragonal structures, obtained by using DFT.

CONCLUSIONS

We have described the first-principles crystal structure prediction based on SA and DFT calculations to search for local minima and the ground state of $LiBH_2$. The present study represents a systematic approach to map the phase space of possible structures thermodynamically accessible, within the accuracy and the limit of the computational approach employed. The recurring topology is the chain formation of the boron hydrogen atoms, which crystal structure can adopt a monoclinic symmetry *Cc* in the ground state by using DFT calculations and orthorhombic *Pnma* by accounting for the dispersion contribution by using Grimme scheme. The monoclinic structure can easily become orthorhombic at the expense of a small amount of energy. In fact, the $-(BH_2)-$ chains show a certain degree of flexibility as highlighted by analyzing the tetragonal symmetry group $P4_322$ (No 95), which is 4.30 kJ/mol higher by using DFT and 2.39 kJ/mol lower by DFT-D than the monoclinic *Cc* structure. The highest energy structures do not show the chain formation, but instead anions $[B_2H_2]^{\delta-}$. In fact, the chain -(BH_2)- gets fragmented as the total energy increases. Limited to four formula units, the modeling approach shows the possibility of ring structure formation, of

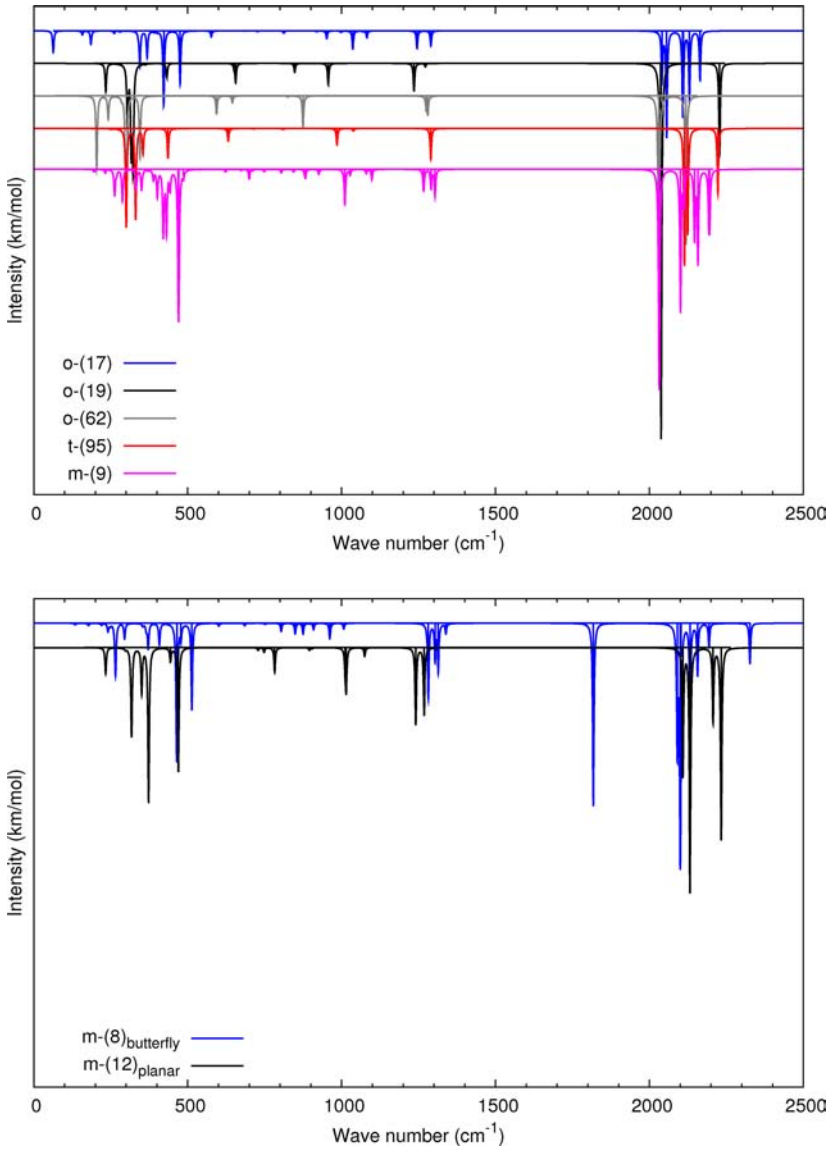

Figure 9. A selection of the simulated IR spectra of the optimized structures: orthorhombic, o-(IT No), tetragonal, t-(IT No), with chain formation, and ring geometry of boron atoms, with monoclinic symmetry, m-(IT No).

dx.doi.org/10.1021/ic301127q | *Inorg. Chem.* 2012, 51, 9757–9765

which the planar square and butterfly configurations are almost isoenergetic, in the limit of DFT calculations, with a reversed trend by using DFT-D. It is highly advisible to have a comparison with possible structures, experimentally achievable, having the stoichiometry $LiBH_2$. Most likely, due to the similarity in the conformations, we might expect a broadening of the experimental diffraction patterns, which might lead one to conclude that $LiBH_2$ eventually does not adopt a crystalline state.

■ ASSOCIATED CONTENT

Supporting Information

Three-dimensional views of the structures containing anionic fragments, view of the chain structure with orthorhombic symmetry, and enthalpy of formation as a function of the molar volume of the optimized structures. This material is available free of charge via the Internet at http://pubs.acs.org.

■ AUTHOR INFORMATION

Corresponding Author

*E-mail: riccarda.caputo@inorg.chem.ethz.ch.

Notes

The authors declare no competing financial interest.

■ ACKNOWLEDGMENTS

Computing resources are provided by the ETH linux cluster, the Inorganic Chemistry Lab, and the National Center for High Performance Computing of Turkey (UYBHM), under the Grant Number 20662009 and Informatics Institute of Istanbul Technical University. Financial support from the SNSF (Sinergia Project CRSII2-130509) is gratefully acknowledged.

■ REFERENCES

(1) Caputo, R.; Züttel, A. *Mol. Phys.* **2010**, *108*, 1263−1276.
(2) Schlesinger, H.; Brown, H. *J. Am. Chem. Soc.* **1940**, *62*, 3429−3435.
(3) Kaufmann, E.; von Ragué Schleyer, P. *Inorg. Chem.* **1988**, *27*, 3987−3992.
(4) Kar, T.; Jug, K. *Chem. Phys. Lett.* **1993**, *214*, 615−620.
(5) Kolmogorov, A.; Drautz, R.; Pettifor, D. *Phys. Rev. B* **2007**, *76*, 184102.
(6) Kang, J. K.; Kim, S. Y.; Han, Y. S.; Muller, R. P.; Goddard, W. A., III *Appl. Phys. Lett.* **2005**, *87*, No. 111904.
(7) Caputo, R.; Tekin, A.; Sikora, W.; Züttel, A. *Chem. Phys. Lett.* **2009**, *480*, 203−209.
(8) Tekin, A.; Caputo, R.; Züttel, A. *Phys. Rev. Lett.* **2010**, *104*, No. 215501.
(9) Caputo, R.; Tekin, A. *J. Solid State Chem.* **2011**, *184*, 1622−1630.
(10) Churchard, A.; et al. *Phys. Chem. Chem. Phys.* **2011**, *13*, 16955−16972.
(11) Dion, M.; Rydberg, H.; Schroder, E.; Langreth, D. C.; Lundqvist, B. I. *Phys. Rev. Lett.* **2004**, *92*, No. 246401.
(12) Thonhauser, T.; Cooper, V. R.; Li, S.; Puzder, A.; Hyldgaard, P.; Langreth, D. C. *Phys. Rev. B* **2007**, *76*, No. 125112.
(13) Tkatchenko, A.; Scheffler, M. *Phys. Rev. Lett.* **2009**, *102*, No. 073005.
(14) Grimme, S. *J. Comput. Chem.* **2006**, *27*, 1787.
(15) Civalleri, B.; Zicovich-Wilson, C. M.; Valenzano, L.; Ugliengo, P. *CrystEngComm.* **2008**, *10*, 405−410.
(16) Bil, A.; Kolb, B.; Atkinson, R.; Pettifor, D. G.; Thonhauser, T.; Kolmogorov, A. *Phys. Rev. B* **2011**, *83*, No. 224103.
(17) Clark, S.; Segall, M.; Pickard, C.; Haspin, P.; Probert, M.; Refson, K.; Payne, M. *Z. Krystallogr.* **2005**, *220*, 567.
(18) Tekin, A.; et al. *Energy Environ. Sci.* **2010**, *3*, 448−456.
(19) Baroni, S.; De Gironcoli, S.; Dal Corso, A.; Giannozzi, P. *Rev. Mod. Phys.* **2001**, *73*, 515−562.